Magnetic structures in the β-TbH(D)$_{2+x}$ system

P. Vajda* and J. N. Daou†
Hydrogène dans les Métaux, Laboratoire de Spectroscopie Atomique et Ionique du CNRS, Bâtiment 350, Université Paris-Sud, F-91405 Orsay, France

G. Andre
Laboratoire Léon Brillouin, Centre d'Etudes Nucléaires de Saclay, F-91191 Gif-sur-Yvette, France
(Received 8 February 1993)

We have measured the electrical resistivity, the susceptibility, and the neutron diffraction spectra of several β-TbH(D)$_{2+x}$ specimens in the range $0 \le x \le 0.245$. The samples present, in general, two magnetic phases at low temperature, one commensurate antiferromagnetic (AF) (phase 2), below $T = T_2$, the other incommensurate AF (phase 1), between T_2 and $T_1 = T_N$, with an overlap region between the two of a relative width $\Delta T/T_2 \sim 0.1$. For the pure dihydride, $x = 0$, the propagation vector of phase 2 is $\mathbf{k}_c = \frac{1}{4}(1,1,3)$ for $T \le T_2 = 16.0$ K, that of phase 1 is $\mathbf{k}_{ic} \sim (0.123,0.137,0.754)$. In the case $x = 0.18$, the phase 2 has a $\mathbf{k}_c = \frac{1}{4}(1,1,4)$ for $T \le T_2 = 32.5$ K and phase 1 a $\mathbf{k}_{ic} \sim (0.25,0.18,1)$. The $\mathbf{k}_{ic}$ for both concentrations vary slightly with temperature in their respective existence ranges $14.8 \le T \le T_1 = 19.0$ K (for $x = 0$) and $29 \le T \le 42$ K for ($x = 0.18$). The magnetic structures for $x = 0.245$ are the same as for $x = 0.18$, the existence ranges shifting to $T \le T_2 = 36$ K and $31 \le T \le T_1 = 42$ K. The magnetic manifestations are very sensitive to possible ordering of the excess hydrogens (x) into an octahedral sublattice of the type DO_{22} occurring around 200 K for $x \gtrsim 0.1$, as evidenced by quenching effects upon the magnetic lines. A magnetic phase diagram in the existence range of the β phase is proposed using the present results and the available data from the literature, showing the disappearance of the phase 2 in the intermediate x range $0.02 \lesssim x \lesssim 0.1$.

I. INTRODUCTION

Like most of the other rare-earth dihydrides, RH_2, TbH_2 crystallizes in the fcc fluorite-type structure (β phase), where the hydrogen atoms occupy ideally all available tetrahedral sites. Additional H atoms x enter the octahedral interstices and interact "ionically" with the lattice-leading to its contraction. The solubility of the x atoms in the β phase decreases, in general, with increasing atomic number Z of the R metal and ranges from $x = 1$ at. H/at. R, in the case of the light R = La, Ce, Pr, to a few at. % H for LuH_{2+x}, before precipitating into the hexagonal trihydride (γ phase). Moreover, the lower β phase boundary as well as its limiting upper value $x^{\beta}_{\max}$ seem to depend critically on the initial metal purity. For high enough amounts of x, from $x \sim 0.10$ on, the excess hydrogens begin to interact with each other repulsively and form a sublattice, which had been observed by various means in several RH_{2+x} systems. For a review of the physical and thermodynamic properties of R-H systems see e.g., a recent compilation by two of the present authors.[1]

In the case of TbH_{2+x}, the solubility limit in the β phase lies in the vicinity of $x^{\beta}_{\max} = 0.25$ at. H/at. Tb and thus permits the observation of ordering phenomena, e.g., as resistivity anomalies in the range of 200 to 300 K.[2,3] At low temperature, TbH_{2+x} orders antiferromagnetically, the magnetic structures and the transition temperatures being strongly dependent on the value of x. Thus, magnetic susceptibility measurements by Arons, Schaefer, and Schweizer[4] on the pure dihydride, $x = 0$ (corresponding to $TbH_{1.95}$ in their case), have shown two transitions: at $T_{N^{\rm I}} = 18.5$ K and at $T_{N^{\rm II}} = 15.8$ K; for $x > 0$, the process at $T_{N^{\rm II}}$ was no longer observable, while $T_{N^{\rm I}}$ shifted progressively to higher temperatures: $T_{N^{\rm I}} = 21$, 26, and 40 K for $x = 0.05$, 0.10, and 0.17, respectively. Heat-capacity measurements[5] exhibited a sharp peak at 16.1 K in the case of $x = 0$ (corresponding to $TbH_{1.93}$ in that experiment) and a small shoulder (not mentioned by the authors) at 18 K; the $x = 0.13$ sample ($TbH_{2.06}$) showed three anomalies: a hump at 24 K, a small but sharp peak at 36.2 K, and another hump at 42 K. Electrical resistivity measurements[3] indicated again two transitions for the $x = 0$ sample ($TbH_{1.96}$): a big drop of $\rho(T)$ at $T_2 \sim 16$ K and a precursor hump near $T_1 \sim 18$ K; with increasing x, both manifestations develop into peaks, T_1 showing generally an increasing tendency while T_2 decreased. But most interesting, for x values where H sublattice ordering did occur (i.e., for $x \gtrsim 0.15$), a quench from room temperature across the ordering anomaly at ~ 200 K modified drastically the magnetic manifestations, strongly increasing the amplitude of the T_2 peak and suppressing the T_1 peak, which clearly showed the correlation between magnetic and structural ordering. Finally, neutron-diffraction measurements on TbD_{2+x}[4,6] have contributed to clarify, at least partly, the situation. Thus, the two transitions in the pure dideuteride ($x = 0$) were attributed to the existence of two phases: an incommensurate intermediate structure between T_1 and T_2 and

a commensurate one modulated along [113] with a period of $4a_0/\sqrt{11}$ (where a_0 is the lattice constant) below T_2. For $x>0$, i.e., $x=0.05$, 0.10, and 0.17, only an incommensurate structure sinusoidally modulated with a propagation vector $\mathbf{k}=(0,0,0.78)$ had been signaled in the literature.[4]

In the following paper, we are presenting results of new detailed neutron-diffraction measurements on the pure dihydride TbD_2 determining, in particular, the structure of the incommensurate phase and establishing a coexistence region of the commensurate and the incommensurate phases. Furthermore, we have investigated specimens with $x>0$, pushing the x values toward the β-phase limit, $x=0.18$ and 0.245, and comparing the neutron-diffraction results with resistivity and susceptibility data. We observe the reappearance of the commensurate structure (which had been lost in previous work[4] for $0<x\leq 0.17$) and propose a magnetic phase diagram, suggesting an interaction between atomic order of the eventually formed x sublattice and the two magnetic configurations.

II. EXPERIMENT

The specimens were prepared from 4*N*-grade Tb metal provided by the Ames Laboratory (Ames, Iowa), containing as main metallic impurities (≥ 2 at. ppm): 12 ppm Fe, 4.5 Ce, 4.2 Cr, 3.5 Pb, 3 W, 3 Cu, 3 Nb, 3 Y, 2.5 Nd, 2 La, 2 Lu. For homogeneity reasons, the hydrogen loading was always performed on bulk specimens: those to be used for neutron diffraction were crushed, after hydrogenation, into powder. Those for resistivity measurements were cut into 20×1 mm^2 platelets of 0.2–1 mm thickness and provided with four spot-welded platinum leads as contacts before hydrogenation; they were broken into pieces after the measurements and used for the susceptibility runs. The loading process itself consisted of two parts: (i) absorption from a calibrated volume of the H quantity needed to form the dihydride by heating at 550°–600°C, giving in our case specimens of the compositions $TbH(D)_{1.96}$ to $TbH(D)_{2.00}$; (ii) the addition of the excess concentration x at 250–300 °C. The very different absorption kinetics of the tetrahedral and the octahedral H atoms guaranteed the clear definition of the x concentration and its determination to a precision of $\pm 1\%$. (The problem has been discussed in detail in Ref. 1). Two of the three specimens studied in neutron diffraction had been deuterated in order to avoid the important incoherent neutron scattering of hydrogen, namely the $x=0$ (pure dideuteride TbD_2) and the $x=0.18$ compositions. The third specimen had been hydrogenated, $x=0.245$ at. H/at. Tb, and was used successively in all three types of experiment for comparison.

The resistivity measurements have been done in a pumped liquid-helium cryostat in the range $1.3\leq T\leq 300$ K, both with decreasing and increasing temperature, using the classical four-point dc method. The magnetic susceptibility was measured by an ac method at a frequency of 500 Hz in an applied static field of $H_0=5$ G.

Neutron-diffraction spectra were collected at the G.41 spectrometer located on a cold-neutron guide position of the Orphée reactor of the Laboratoire Léon Brillouin at Saclay, using an 800 cell multidetector covering the range $2°\leq 2\Theta\leq 82°$. The employed neutron wavelength was $\lambda=2.439$ Å and the investigated temperature interval $1.5\leq T\leq 300$ K. A quenching procedure was applied to study the role of H sublattice ordering by dipping the sample holder into liquid nitrogen before its transfer into the liquid-helium cryostat, the quenching rate varied between ~ 5 and 50 K/min. The obtained spectra were analyzed by comparing the observed integrated intensities with the calculated ones by means of a program.

III. EXPERIMENTAL RESULTS

A. Electrical resistivity

In Fig. 1, we are presenting electrical resistivity data obtained on a series of TbH_{2+x} specimens. The pure $x=0$ dihydride is drawn for comparison and is taken over from earlier work;[3] $\rho(T)$ shows the strong drop at $T_N(=T_2)$, followed at higher temperatures by the essentially linear phonon contribution. (The hump at $T_1\sim 18$ K mentioned in Sec. I is not visible in this plot.)

Adding x hydrogens on octahedral sites modifies the aspect of the $\rho(T)$ curves qualitatively. First, the low-temperature, magnetic part develops a maximum near 12 K (LT peak), for $x=0.07$; it is followed by a second maximum near 38 K (HT peak), for the three samples with $0.15\leq x\leq 0.20$, the latter peak growing with increasing x and the former decreasing simultaneously. For the $x=0.245$ specimen, the LT peak has vanished and the HT maximum has become a huge, λ shaped structure peaking at 40 K. As already suggested earlier,[3] these

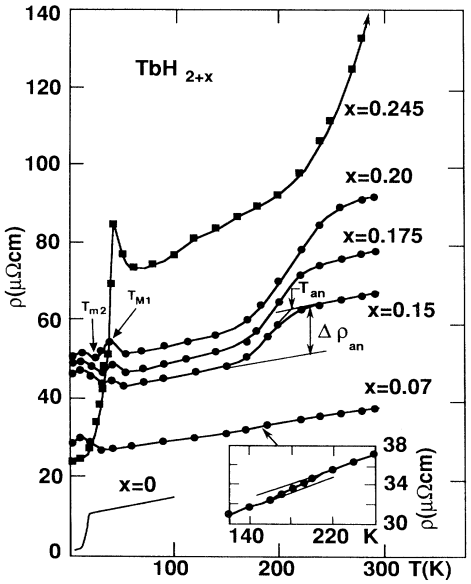

FIG. 1. Thermal dependence of the electrical resistivity of various TbH_{2+x} specimens, with $0\leq x\leq 0.245$, indicating the temperatures for structural T_{an}, and magnetic T_{m2}, T_{M1}, transformations (see text). The inset gives an enlarged view of the structural anomaly region for the $x=0.07$ sample. The curve for $x=0$ has been taken over from Ref. 3.

peaks can be discussed in terms of commensurate and incommensurate magnetic phases.

As concerns the origin and the evolution of these phases, a first phenomenological interpretation can be given from an analysis of the $\rho(T)$ behavior above $T\sim 150$ K. One notes the clear evolution of an anomaly superimposed upon the phononic part and centered around 200 K. Both the amplitude of the anomaly $\Delta\rho_{an}$ and the anomaly temperature T_{an} defined as its high-T end (as shown in Fig. 1), increase with increasing x; it is just present for $x=0.07$ (see inset), and is so strongly developed for $x=0.245$ that it has not yet reached its upper end at room temperature. This anomaly has the typical form for the expression of a structural transformation mechanism and has been assigned to x sublattice ordering. It shall be shown later in this paper in the neutron-diffraction analysis, but is also manifest in the anomalous thermal behavior of the lattice parameter as determined by x-ray diffraction.[7]

B. Magnetic susceptibility

The $x=0.245$ specimen of the resistivity run was used subsequently for a magnetic-susceptibility measurement. We are showing in Fig. 2 the low-temperature region, which exhibits magnetic ordering. One notes the end of the paramagnetic phase at $T=T_1\sim 50$ K, followed by a linear part roughly 10 K wide and a strong drop centered at 39 K going over into a flatter T dependence toward 4 K. It is clear that at least two magnetic transitions are visible in the susceptibility curve, in contrast to the results of Ref. 4, where the authors had seen only one transition for $x>0$, with a maximum value for $T_N=40$ K in the case of $x=0.17$. Thus, it is tempting to assign the region between 40 and 50 K to the incommensurate phase and the drop at 39 K to the transition toward the commensurate AF phase. This seems reasonable in view of the analogy with the two-peak structure of the resistivity curves for TbH_{2+x} with $0.15\le x\le 0.20$, despite the absence of the LT peak in the $\rho(T)$ curve for the $x=0.245$ sample; the drop at 40 K in the latter case is probably too steep to make the emergence of a small LT peak visible.

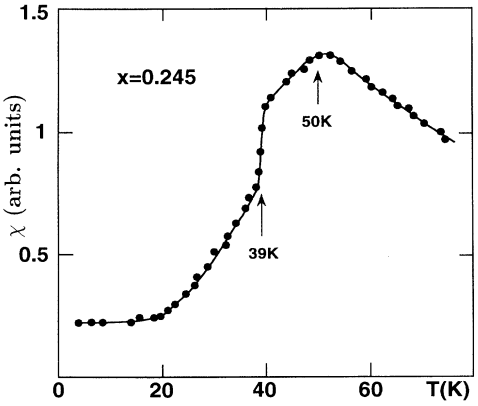

FIG. 2. ac susceptibility in a static field $H_0\sim 5$ G as a function of temperature for $TbH_{2.245}$, indicating two magnetic transitions.

We shall see this confirmed in the next section on neutron diffraction.

C. Neutron diffraction

1. $TbD_{2.00}$

The pure dideuteride ($x=0$), as defined by the preparation procedure described in Sec. II, had the concentration $TbD_{2.00(1)}$, the nominal x values for the excess H concentrations are, therefore, also the real ones when compared with earlier work.[4,6] The spectra were taken at 16 different temperatures between 1.8 and 50 K in order to cover the whole magnetically ordered range and, in addition, to attain an interval where the $x>0$ specimens, too, exhibit ordering (cf. the following subsections). Figure 3 shows a selection of spectra between 1.8 and 25 K displaying two distinct magnetic phases.

a. Phase 2. Besides the nuclear lines (111) and (200) present at all temperatures, one observes below $T_2=16.0$ K magnetic lines corresponding to a commensurate antiferromagnetic structure of wave vector $\mathbf{k}=\frac{1}{4}(1,1,3)$, in complete agreement with the data of Arons, Schaefer, and Schweizer[4] and Shaked *et al.*[6] The magnetic moment of the Tb ion is parallel to the c axis and is determined to $|\mu|=7.55(20)\mu_B$ at 1.8 K, as compared to the $7.4(4)\mu_B$ given in Ref. 6. The reliability factor is $R_{mag}=2.4\%$, reflecting the high quality of the spectra [Fig. 4(a)]. The temperature dependence of the magnetic moment of this phase is shown in Fig. 5.

b. Phase 1. Another magnetic phase is observed in the interval $14.8\le T\le 19.0$ K, overlapping the existence region of phase 2 by 1.2 K. Its peak intensities are max-

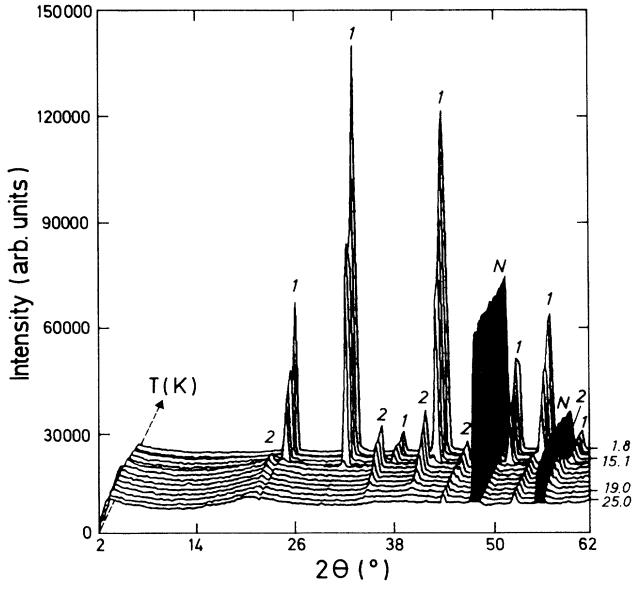

FIG. 3. Global view of the neutron-diffraction spectra of $TbD_{2.00}$ at various temperatures in the magnetically ordered region. Note the overlapping existence ranges for the commensurate (1) and incommensurate (2) AF phases. N: nuclear reflections.

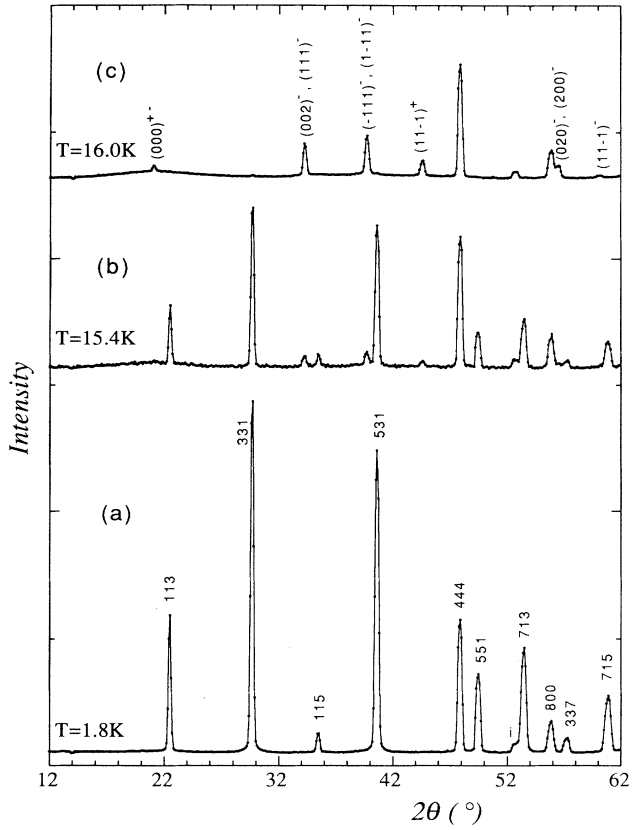

FIG. 4. Neutron-diffraction spectra of $TbD_{2.00}$ at different temperatures. (a) $T=1.8$ K, showing the commensurate phase only; (b) $T=15.4$ K, coexistence of both phases; (c) $T=16.0$ K, incommensurate phase only. (i) impurity in the sample environment.

imum at $T=16.0$ K and the corresponding spectrum is exhibited in Fig. 4(c); the coexistence of both phases 1 and 2 is shown in Fig. 4(b). Phase 1 had already been noted as "intermediate structure" in the work by Shaked *et al.*,[6,8] but had not been indexed by them due to weak intensities and the low number of characteristic peaks. We have determined this structure as incommensurate antiferromagnetic (AF), with a propagation vector **k** varying with temperature, such that, e.g., at $T=16.0$ K, one has $\mathbf{k}=(0.123, 0.137, 0.754)$ and, at 17.3 (0.122, 0.136, 0.753) implying a slight but significant increase of the modulation period with increasing T. The magnetic moment remains parallel to the c axis, its value is $|\mu|=2.8\mu_B$ at 16.0 K, the temperature variation is shown together with that of phase 2 in Fig. 5. The observed and calculated integrated intensities at $T=16.0$ K are given in Table I, yielding a reliability factor $R_{\text{mag}}=8.0\%$. The structures of phase 1 and phase 2 are drawn in Fig. 6.

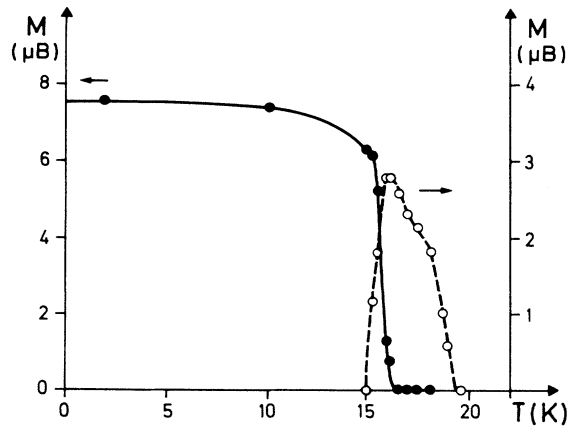

FIG. 5. Temperature dependence of the magnetic moments in $TbD_{2.00}$ for both AF phases. filled circles: phase 2; open circles: phase 1. Note the different ordinate scales.

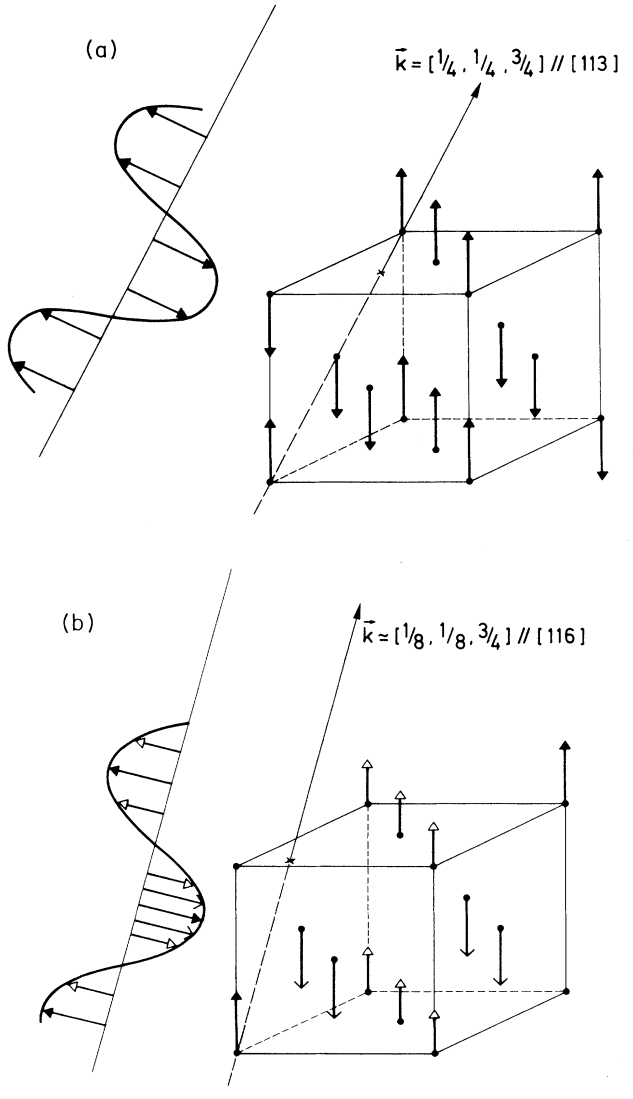

FIG. 6. Magnetic structures of the commensurate phase (2), Fig. 6(a), and of incommensurate phase (1), Fig. 6(b), and the projections of their moments upon the directions of the corresponding propagation vectors in $TbD_{2.00}$. For the relative sizes of the moments in the two phases, see Fig. 5.

TABLE I. Observed and calculated integrated intensities of $TbD_{2.00}$ at 16 K.

hkl	I_{calc}	I_{obs}
$000(\pm)$	15	17
$002^{(-)}$, $111^{(-)}$	94	96
$-111^{(-)}$, $1-11^{(-)}$	134	123
$11-1^{(+)}$	53	58
$020^{(-)}$, $200^{(-)}$	55	54
$11-1^{(-)}$	9	9
$-202^{(-)}$, $02-2^{(+)}$	29	34
$220^{(-)}$	14	21

2. $TbD_{2.18}$

The specimen with $x=0.18$ exhibits a nuclear transition in the region between 200 and 270 K, whose manifestation has been noted in the electrical resistivity curves (Fig. 1); the slightly higher transition interval is probably partly due to an isotope effect. The low-temperature nuclear structure has been analyzed in a companion paper,[9] together with other excess hydrogen concentrations in the range $0.10 \leq x \leq 0.18$; a structural phase diagram had been presented. It was attributed to hydrogen sublattice ordering in a DO_{22} structure of the Ni_3Mo-type, with the interstitial (420) planes in the fcc structure organized in such a way that every three empty planes were followed by one filled. The superlattice reflections (see the spectrum at $T=67$ K in Fig. 7) can be indexed in the tetragonal $I4/mmm$ system. A reliability factor $R_N=7.6\%$ was obtained assuming $\sim 80\%$ of the octahedral H atoms ordered in the DO_{22} structure and $\sim 20\%$ distributed statistically in the remaining sites.

18 spectra were taken with this specimen in the temperature range $1.4 \leq T \leq 230$ K and have also exhibited two magnetic phases at low temperatures; this is in agreement with the resistivity data (Fig. 1 and Ref. 3) but in contrast to the results of Arons, Schaefer, and Schweizer[4] whose equivalent $TbD_{2.12}(=TbD_{1.95+0.17})$ specimen had shown only one transition near 40 K.

a. Phase 2. This phase is present below $T_2=32.5$ K and has not been signaled in the work by Arons, Schaefer, and Schweizer;[4] on the other hand, the transition temperature seems to correspond to the first minimum observed in the resistivity of the $x=0.175$ sample (Fig. 1). The spectrum at 1.4 K is shown in Fig. 8(a).

The structure is AF commensurate, with a propagation vector $\mathbf{k}=\frac{1}{4}(1,1,4)$, i.e., *different* from the low-temperature phase in the $TbD_{2.00}$ specimen.

Quench effects: The presence of an ordered hydrogen sublattice below a temperature of ~ 200 K has incited us to investigate an eventual prevention of its ordering by quenching the sample into liquid nitrogen. Two different cooling rates were applied; a semirapid rate of about 20

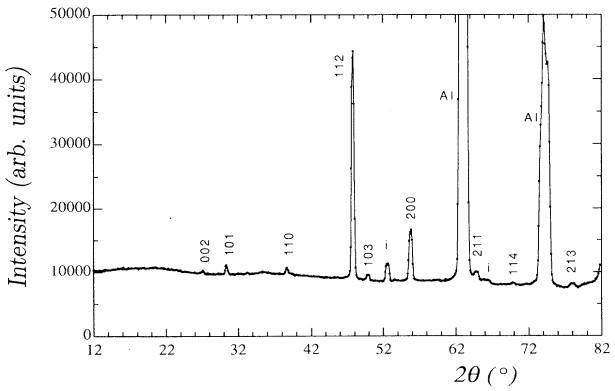

FIG. 7. Neutron-diffraction spectrum of $TbD_{2.18}$ at $T=67$ K, showing the superlattice lines of the ordered hydrogen configuration, indexed according to the tetragonal unit cell $(a,a,2a)$. i represents the impurity in the sample environment.

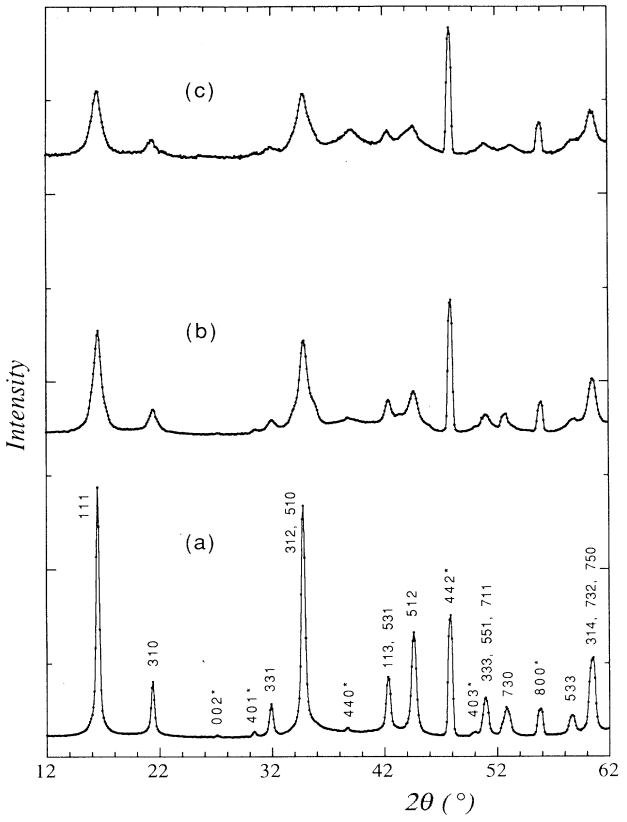

FIG. 8. Neutron-diffraction spectrum of $TbD_{2.18}$ in the commensurate phase at $T=1.5$ K, showing the influence of a quenching treatment upon the magnetic and the structural superlattices. (a) after slow cooling (≤ 1 K/min cooling rate); (b) after a semirapid quench (~ 5 K/min); (c) after a rapid quench (~ 50 K/min). (*) nuclear superlattice peaks.

min for the interval 300 to 160 K, and a rapid rate of ~ 3 min for the same T range. The spectra taken at 1.4 and 1.6 K are exhibited in Figs. 8(b) and 8(c), respectively, and show an increasing broadening of the magnetic and the superstructure lines. The (002) and (101) lines of the latter have practically disappeared after a quench (as seen in the enlarged part of the spectra between $2\Theta = 26°$ and 33° in Fig. 9), indicating the nearly complete destruction of the x hydrogen sublattice. It has to be noted, moreover, that even for the slowly cooled specimens ($\lesssim 1$ K/min cooling rate) both the magnetic and the superstructure lines are somewhat broadened at the foot compared to the main structural nuclear lines (112) and (200), showing the presence of some disorder [see Fig. 8(a)]; as mentioned above, the best fit to the observed spectrum was obtained by assuming $\sim 20\%$ of the x atoms as disordered.

b. Phase 1. Another magnetic phase is observed in the interval 29 K $\leq T \leq$ 42K, also overlapping with phase 2 (as for $x=0$) but, this time, by 3.5 K. The transition temperature towards the paramagnetic region, $T_1 = 42$ K, corresponds nicely to the $T_N = 40$ K given by Arons, Schaefer, and Schweizer[4] for their $TbD_{2.12}$ sample and to the high-temperature peak in resistivity as shown in Fig. 1. The diffraction spectrum for a temperature of 33 K is exhibited in Fig. 10 and indicates again abnormal broadening at the foot of the magnetic and superstructure lines, probably due to incomplete ordering of the H sublattice. The structure of phase 1 is incommensurate

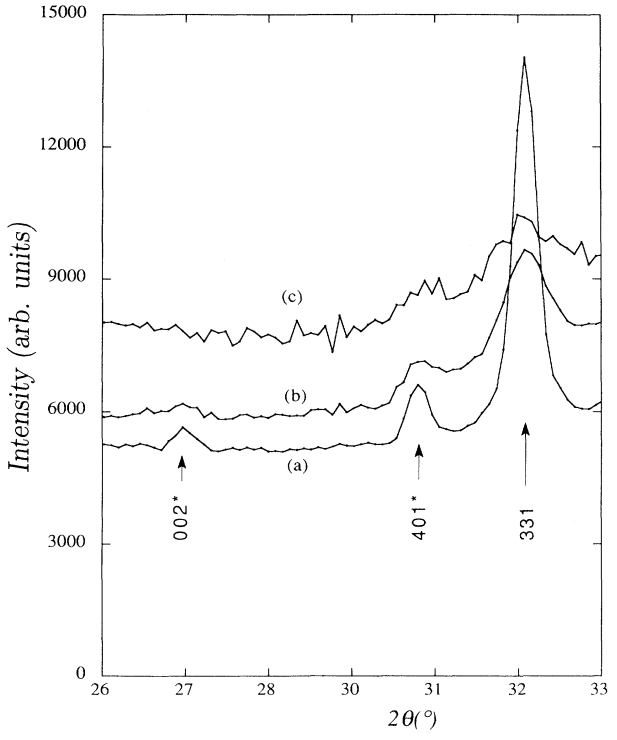

FIG. 9. Enlarged part of Fig. 8. Evolution of the hydrogen superstructure lines (002)* and (401)*, indexed in the cubic unit cell, and of the magnetic superstructure lines (331M) of $TbD_{2.18}$ at $T = 1.5$ K after a quench treatment.

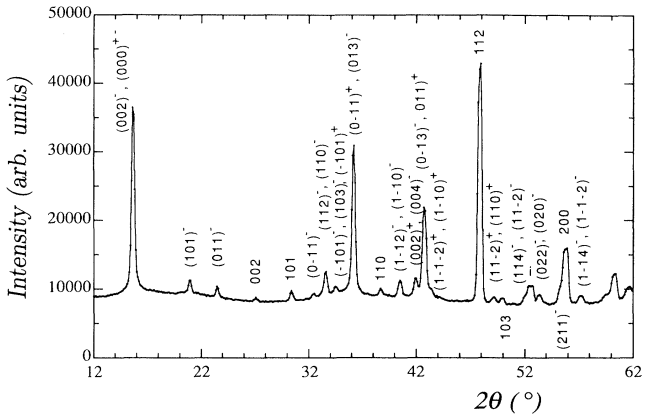

FIG. 10. Neutron-diffraction spectrum of $TbD_{2.18}$ in the incommensurate phase at $T = 33$ K.

AF, with a propagation vector varying within the existence range; typical values are

at $T = 30$ K: $\mathbf{k} = (0.250, 0.180, 1)$,

at $T = 33$ K: $\mathbf{k} = (0.243, 0.165, 1)$,

at $T = 40$ K: $\mathbf{k} = (0.238, 0.157, 1)$.

One notes the same tendency toward an increasing modulation period with increasing T as for phase 1 in $TbD_{2.00}$, easier to detect here due to the wider stability range.

The quenching treatment discussed in the previous subsection was also analyzed for the incommensurate phase (at 33.0 K) and resulted in analogous effects; increased broadening of magnetic and superstructure lines accompanied by a growing background.

3. $TbH_{2.245}$

The specimen used in this study was the same as that used in resistivity and susceptibility measurements (Figs. 1 and 2). The use of hydrogen instead of deuterium increased the background but the superstructure lines of the DO_{22} configuration are still visible at low temperature (Fig. 11). No quench experiments had been undertaken on this specimen, but we do not expect a significant modification of the spectra in view of the fact that the ordering transformation already begins above room temperature (cf. Fig. 1); trial experiments had shown the presence of the superstructure lines also at room temperature. It is interesting to note in this context that the lattice parameter a determined by x-ray diffraction in the system β-TbH_{2+x} by two of the present authors[7] shows, for $x = 0.24$, a marked change of slope da/dT around $T = 180$ K, indicating a change in the electronic structure of the metal sublattice. Since this critical temperature is situated just at the end of the transformation stage as seen by resistivity (Fig. 1), we have here a clear sign of the influence of H sublattice ordering upon the metal lattice.

The magnetic phases are the same as for the $TbD_{2.18}$ specimen, but with an enlarged existence region. Thus,

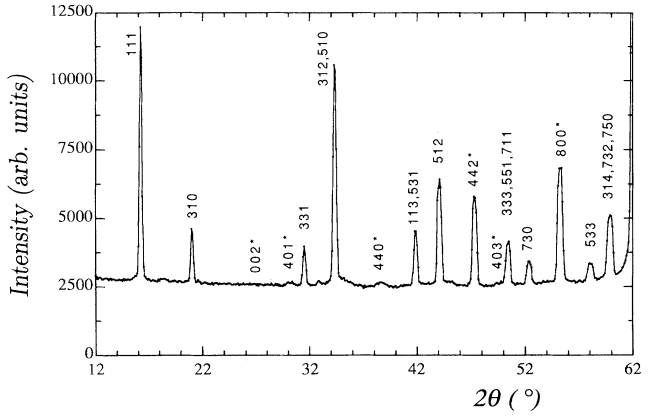

FIG. 11. Neutron-diffraction spectrum of $TbH_{2.245}$ at $T=1.5$ K, showing the commensurate phase and traces of the hydrogen superstructure lines.

phase 2 is present below $T_2=36$ K and phase 1 between 31 and 42 K, the coexistence interval between the two phases being $\Delta T=5$ K.

The transition temperature towards paramagnetism, $T_1=42$ K, is in excellent agreement with the peak temperature of 42 K in resistivity (Fig. 1), while the transition incommensurate-commensurate at 36 K is not visible on the ρ curve of Fig. 1, probably because of its very steep drop. On the other hand, two transitions are also observable in the magnetic susceptibility (Fig. 2), though their temperatures seem shifted to higher values by several degrees.

D. Other concentrations

Qualitative investigations in the magnetically ordered region of several intermediate concentrations performed on the triple-axis spectrometer Valse at the same neutron guide (cf. Ref. 9) indicated, for $x=0.08$, just an incommensurate phase with a propagation vector $\mathbf{k}=(0,0,0.77)$, and, for $x=0.11$, the same phases as for $x=0.18$.

IV. DISCUSSION

The most important result of the present investigation is the confirmation of the suggestion made from electrical resistivity studies[3] of a relation between magnetic ordering of the Tb moments and hydrogen sublattice ordering on octahedral (x) sites. The presence of an ordered H sublattice above a concentration of $x\gtrsim 0.1$ at low temperature[9] leads to the lowering of the crystal-field symmetry (probably from cubic to tetragonal in view of the DO_{22} structure for the ordered configuration), which, in its turn, can lead to a change of the magnetic manifestations. On the other hand, the modifications introduced by H sublattice ordering might be of an even more fundamental nature leading to changes in the Fermi-surface nesting topology, as indicated by experiments on the β-GdH_{2+x} system,[10] where the crystal-field role was negligible because of the S character of the Gd ion ground state.

Similar crystal-field considerations had been made by Drulis, Opyrchal, and Borkowska,[5] who attempted to interpret their specific-heat data on $TbH_{2.06}(=TbH_{1.93+0.13})$ through a reduction of the cubic symmetry to axial by the presence of octahedral H atoms; they did not, however, take into account a possible ordering of these H atoms, which should already have taken place for $x=0.13$. Similarly, Arons, Schaefer, and Schweizer[4] had suggested that the transition from commensurate to incommensurate magnetic structure for $x>0$ was related to the presence of octahedral H atoms; they had not considered, however, the H sublattice ordering and the reappearance of commensurate magnetism for $x\gtrsim 0.1$.

We are proposing in Fig. 12 a magnetic phase diagram constituted from our neutron-diffraction and susceptibility data, the resistivity data from this work and Ref. 3, the susceptibility and neutron data from Ref. 4, and from specific-heat data.[5] The respective x values from Ref. 4 and 5 were adjusted such as to be able to relate them to their "pure" dihydride. The critical temperatures for the resistivity data are the HT peak at T_{M1} and the LT minimum at T_{m2} (cf. Fig. 1), with an inherent uncertainty due to superposition of the phonon contribution. The essential observation in this phase diagram is the presence of several transitions for low and for high x values, separated by a domain with only one transition for intermediate x.

As to the magnetic structures themselves, it is encouraging that the two commensurate configurations (a) and (b) are *not* identical, one with a propagation vector $\mathbf{k}=\frac{1}{4}(1,1,3)$, the other with $\mathbf{k}=\frac{1}{4}(1,1,4)$, in view of the presence of different H order in the two cases. The same is also true for the incommensurate configurations, though there the variation is more complicated, having the temperature as an additional parameter. Furthermore, let us mention, in this context, the presence of two

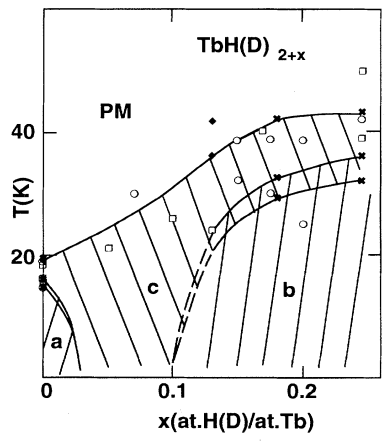

FIG. 12. Magnetic phase diagram of $TbH(D)_{2+x}$, exhibiting the existence regions for the two commensurate phases (a) and (b) and the incommensurate phase (c). ×, neutron data, this work; ○, resistivity data from Fig. 1, using T_{M1} and T_{m2}, and from Ref. (3); □, susceptibility data from Fig. 2 and from Refs. 4 and 5; ◆, specific-heat data from Ref. 5.

types of Tb atoms with regard to their surroundings in an ordered DO_{22} structure: 25% of them have two occupied octahedral H sites as nearest neighbors and 75% only one, thus giving a nice indication for the different crystal-field symmetries as a possible origin of the various magnetic phases.

Finally, we want to mention the observation of a coexistence region of the two, commensurate and incommensurate, magnetic phases. It looks as if the *ic* structure were somehow a precursor for the regular commensurate configuration, which stabilizes at low temperature, and coexists with the latter during a certain interval ΔT; it is interesting to note the nearly constant relative width of the coexistence interval, $\Delta T/T_2 \approx 0.1$, for all x values measured, implying the same phenomenon at its origin.

V. SUMMARY

We have investigated the magnetic structures observed at low temperatures in the system β-TbH(D)$_{2+x}$ for the concentrations $x=0$, 0.18, and 0.245. For each case, there exist two magnetic configurations, one below $T=T_2$, which is commensurate with the lattice, the other between T_2 and T_1, which is incommensurate and whose propagation vector varies with the temperature; a narrow coexistence region of a width $\Delta T/T_2 \approx 0.1$ is observed for the two magnetic phases. The eventual ordering of the excess hydrogen atoms on octahedral sites into a sublattice, for values of $x \gtrsim 0.1$, has a striking influence upon the magnetic manifestations, increasing their transition temperatures and modifying the configurations of the magnetic phases.

A magnetic phase diagram for β-TbH(D)$_{2+x}$ is proposed, taking into account the available neutron-diffraction data and the relevant resistivity, susceptibility, and heat-capacity results. In view of qualitatively similar low-temperature behavior of other magnetic rare-earth hydrides β-RH$_{2+x}$ (see, e.g., Ref. 1), we suggest for them an analogous correlation mechanism between x hydrogen ordering and magnetism, which is to be studied by neutron scattering.

ACKNOWLEDGMENTS

We wish to thank A. Boukraa, O. Blaschko, and W. Schwarz for useful discussions.

---

*Also at Laboratoire des Solides Irradiés, Ecole Polytechnique, F-91128 Palaiseau, France.

†Deceased.

[1] P. Vajda and J. N. Daou, in *Hydrogen-Metal Systems,* edited by A. Aladjem and F. A. Lewis (VCH Weinheim, Germany, 1993), Vol. 1, Chap. 3a.

[2] J. N. Daou, P. Vajda, J. P. Burger, and A. Lucasson, Phys. Status Solidi A **98**, 183 (1986).

[3] P. Vajda, J. N. Daou, and J. P. Burger, Phys. Rev. B **36**, 8669 (1987).

[4] R. R. Arons, W. Schaefer, and J. Schweizer, J. Appl. Phys. **53**, 2631 (1982).

[5] M. Drulis, J. Opyrchal, and W. Borkowska, J. Less-Common Met. **101**, 211 (1984).

[6] H. Shaked, D. G. Westlake, J. Faber, and M. H. Mueller, Phys. Rev. B **30**, 328 (1984).

[7] M. Chiheb, J. N. Daou, and P. Vajda, *International Symposium on Metal-Hydrogen Systems, Uppsala, Sweden, 1992* [Z. Phys. Chem. **178** (1993)].

[8] H. Shaked, J. Faber, M. H. Mueller, and D. G. Westlake, Phys. Rev. B **16**, 340 (1977).

[9] G. André, O. Blaschko, W. Schwarz, J. N. Daou, and P. Vajda, Phys. Rev. B **46**, 8644 (1992).

[10] P. Vajda, J. N. Daou, and J. P. Burger, J. Less-Common Met. **172-174**, 271 (1991).